

Xrcc1-dependent and Ku-dependent DNA double-strand break repair kinetics in Arabidopsis plants

Cyril Charbonnel, Maria E. Gallego and Charles I. White*

Génétique, Reproduction et Développement, UMR CNRS 6247 – Clermont Université – INSERM U931, Université Blaise Pascal, UFR Sciences et Technologies, 24 Avenue des Landais, BP 80026, 63171 Aubière Cedex, France

Received 31 May 2010; revised 23 July 2010; accepted 30 July 2010; published online 8 September 2010.

*For correspondence (fax +33 473 407 777; e-mail chwhite@univ-bpclermont.fr).

SUMMARY

Double-strand breakage (DSB) of DNA involves loss of information on the two strands of the DNA fibre and thus cannot be repaired by simple copying of the complementary strand which is possible with single-strand DNA damage. Homologous recombination (HR) can precisely repair DSB using another copy of the genome as template and non-homologous recombination (NHR) permits repair of DSB with little or no dependence on DNA sequence homology. In addition to the well-characterised Ku-dependent non-homologous end-joining (NHEJ) pathway, much recent attention has been focused on Ku-independent NHR. The complex interrelationships and regulation of NHR pathways remain poorly understood, even more so in the case of plants, and we present here an analysis of Ku-dependent and Ku-independent repair of DSB in *Arabidopsis thaliana*. We have characterised an *Arabidopsis xrcc1* mutant and developed quantitative analysis of the kinetics of appearance and loss of γ -H2AX foci as a tool to measure DSB repair in dividing root tip cells of γ -irradiated plants *in vivo*. This approach has permitted determination of DSB repair kinetics *in planta* following a short pulse of γ -irradiation, establishing the existence of a Ku-independent, Xrcc1-dependent DSB repair pathway. Furthermore, our data show a role for Ku80 during the first minutes post-irradiation and that Xrcc1 also plays such a role, but only in the absence of Ku. The importance of Xrcc1 is, however, clearly visible at later times in the presence of Ku, showing that alternative end-joining plays an important role in DSB repair even in the presence of active NHEJ.

Keywords: Xrcc1, Ku80, double-strand break (DSB) repair, non-homologous recombination, gamma-H2AX, kinetics.

INTRODUCTION

The DNA of living cells is subject to damage, and this must be repaired in order to preserve the information stored in the genome. Double-strand breakage (DSB) of DNA is particularly deleterious, involving loss of information on the two strands of the DNA fibre and thus precluding the simple copying of the complementary strand that is possible in the repair of single-strand DNA damage. In diploid (or polyploid) organisms, or in post-replicative phases of the cell cycle in haploids, repair processes based on homologous recombination can precisely repair the DSB using another copy of the genome as template (reviewed by San Filippo *et al.*, 2008). The prevalence of dispersed repeated DNA sequences in eukaryotic genomes, however, complicates this, permitting the use of non-allelic DNA sequences as a template for repair. Crossing-over associated with such ectopic homologous recombination using non-allelic templates carries the risk of generating major genome rearrangements and thus

requires careful control (Sonoda *et al.*, 2006; San Filippo *et al.*, 2008; Shrivastav *et al.*, 2008; Mimitou and Symington, 2009).

In addition to homology-based mechanisms, non-homologous recombination (NHR) permits repair of DSB with little or no dependence on DNA sequence homology (reviews by Lieber, 2010; Mahaney *et al.*, 2009). The first NHR pathway to have been described is Ku-dependent canonical non-homologous end-joining (C-NHEJ). This pathway involves recognition of the broken DNA ends by the Ku heterodimer (Ku70 and Ku80, or Ku86 in mammals), binding of DNA PKcs (specific to vertebrates), Artemis and X-family polymerases, followed by XLF, Xrcc4 and DNA ligase IV to seal the gap. In addition, numerous studies of the C-NHEJ pathway have revealed the existence of alternative end-joining mechanisms among the three eukaryote kingdoms (Kramer *et al.*, 1994; Liang *et al.*, 1996; Moore and Haber, 1996; Feldmann

et al., 2000; Guirouilh-Barbat *et al.*, 2004). Ku-independent end-joining pathways produce different types of joints, in particular involving the use of microhomologies and the generation of larger deletions at the joint. Microhomology-mediated end-joining (MMEJ) was first described in yeast and requires the Mre11–Rad50–Xrs2 complex and the structure-specific endonuclease Rad1–Rad10 (Ma *et al.*, 2003; Zhang and Paull, 2005). The role of the Xpf–Ercc1 (yeast Rad1–Rad10) and the Mre11–Rad50–Nbs1 (MRN) complex in Ku-independent end-joining has also been confirmed in vertebrates (Ahmad *et al.*, 2008; Rass *et al.*, 2009; Taylor *et al.*, 2009; Xie *et al.*, 2009). Moreover, a number of studies have shown the implication of the single-strand break repair (SSBR) proteins in a Ku-independent end-joining pathway: Parp1, Xrcc1, DNA ligase III α or DNA ligase I (Gottlich *et al.*, 1998; Audebert *et al.*, 2004; Wang *et al.*, 2005; Liang *et al.*, 2008). Parp1, Xrcc1 and DNA ligase III α are sufficient to promote end-joining *in vitro* and show a preference for the use of terminal microhomologies for the repair of the break (Audebert *et al.*, 2004, 2008; Wang *et al.*, 2006; discussed by Nussenzweig and Nussenzweig, 2007). Recent publications indicate that C-NHEJ acts to avoid the use of these alternative end-joining pathways (Boboila *et al.*, 2010; Fattah *et al.*, 2010; Simsek and Jasin, 2010). The distinction drawn between the Ku-independent end-joining pathways, alternative NHEJ (A-NHEJ) and MMEJ, is not clear at this time and they are often grouped under the single heading of alt-NHEJ.

The C-NHEJ core proteins, Ku80, Ku70, Xrcc4 and DNA ligase IV, have been described in plants (West *et al.*, 2000, 2002; Riha *et al.*, 2002; Tamura *et al.*, 2002; van Attikum *et al.*, 2003; Friesner and Britt, 2003; Gallego *et al.*, 2003; Kozak *et al.*, 2009). *Arabidopsis ku80*, *ku70* and *lig4* mutant plants are hypersensitive to DSB-inducing reagents and absence of the AtKu80 protein has been shown to reduce the efficiency of NHEJ in an *in vivo* plasmid-based end-joining assay (Gallego *et al.*, 2003). The identification of the *Arabidopsis Xrcc4* has been confirmed by two-hybrid and coimmunoprecipitation experiments, showing its interaction with the AtLig4 protein (West *et al.*, 2000). No plant orthologue of XLF has been described thus far; however, concerning Artemis, the genome of *Arabidopsis* encodes three SNM-like proteins (Molinier *et al.*, 2004) and the *Arabidopsis* DNA ligase VI gene has a predicted β -CASP motif (Bonatto *et al.*, 2005). Much less is known about the alt-NHEJ pathways in *Arabidopsis*. No ligase III orthologue has been identified in *Arabidopsis*, although it has three identified DNA ligases and it is likely that DNA ligase I (Waterworth *et al.*, 2009) or the plant-specific DNA ligase VI (Bonatto *et al.*, 2005) may fulfil this role. Plants have putative Xrcc1 orthologues (Taylor *et al.*, 2002; Uchiyama *et al.*, 2008). The rice protein (OsXRCC1) has been shown to bind single-stranded (ss)- and double-stranded (ds)-DNA and to interact with PCNA *in vivo* (Uchiyama *et al.*, 2008), and the

Arabidopsis Xrcc1 protein stimulates repair of uracil in DNA in a cell-free assay (Cordoba-Canero *et al.*, 2009). Parp1 and Parp2 orthologues are also present in plants, and although no direct role has as yet been shown in base excision repair (BER), their transcription is induced by oxidative stress and IR, they localise to the nucleus and their poly-ADP-ribosylation activities are activated by DNA strand breaks (Babiychuk *et al.*, 1998; Doucet-Chabeaud *et al.*, 2001; Lepiniec *et al.*, 1995; review by Roldan-Arjona and Ariza, 2009). As mentioned above, a study of end-joining in a plasmid DNA transformation assay showed that in *ku80* mutant cells, a Ku80-independent pathway was able to carry out a quarter to a half of the end-joining detected in the wild type (Gallego *et al.*, 2003). Also, absence of Mre11 resulted in reduced usage of microhomologies in a study of chromosome fusions in *ku70 tert* mutant *Arabidopsis* (Heacock *et al.*, 2004).

Although knowledge of the mechanisms of these different NHR pathways has considerably advanced in recent years, the complex interrelationships and regulation of NHR are far from being fully understood. This is even more the case in plants (Bleuyard *et al.*, 2006), and we present here an analysis of Ku-dependent and Ku-independent repair of DSB in the plant *Arabidopsis thaliana* using *atku80* and *xrcc1* mutants. Xrcc1 is a key protein in BER and SSBR, acting as a scaffold for other DNA repair proteins (reviews by Caldecott, 2003; Roldan-Arjona and Ariza, 2009). Two recent *in vitro* studies, in rice (Uchiyama *et al.*, 2008) and *Arabidopsis* (Cordoba-Canero *et al.*, 2009), have confirmed the functional role of this protein in BER in plants and we present here the characterisation of an *Arabidopsis xrcc1* mutant and analysis of the role of the AtXrcc1 and AtKu80 proteins in DSB repair *in planta*. We have developed analysis of the kinetics of appearance and loss of γ -H2AX foci as a tool to measure DSB repair kinetics in dividing root tip cells of irradiated plants *in vivo*. This approach has permitted us to determine DSB repair kinetics *in planta* following a short pulse of γ -irradiation, and shows the existence of a Ku-independent, Xrcc1-dependent DSB repair pathway in *Arabidopsis*.

RESULTS

Identification of an *Arabidopsis xrcc1* mutant

The XRCC1 orthologue of *Arabidopsis thaliana* lies on chromosome I at locus *At1G80420* (Taylor *et al.*, 2002; Uchiyama *et al.*, 2008). Screening of the *Arabidopsis* T-DNA insertion mutant collection (Alonso *et al.*, 2003) via the Salk Institute site (<http://signal.salk.edu/cgi-bin/tdnaexpress>) permitted the identification of a putative *xrcc1* mutant line (Salk_027362). T₃ seed from this line was obtained from the Nottingham *Arabidopsis* Stock Centre (Scholl *et al.*, 2000) and wild-type, heterozygote and homozygote plants for the insertion allele *xrcc1* were identified by PCR genotyping (see Experimental Procedures). *xrcc1* mutant plants are fertile

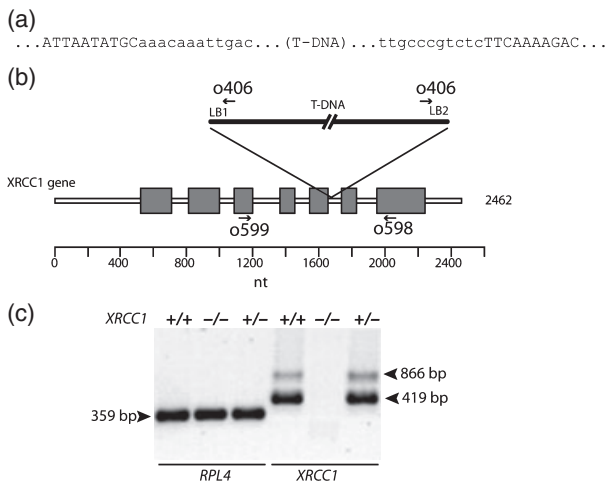


Figure 1. Characterisation of an *xrcc1* mutant line.

(a) Sequence at the borders of the T-DNA insertion: uppercase letters are the *XRCC1* gene sequence, lowercase letters are the T-DNA sequence. A three nucleotide deletion (TCT) of the *XRCC1* gene occurred at the T-DNA insertion site.

(b) Structure of the *XRCC1* gene with exons (grey boxes), the positions of the insertion and of the primers used for PCR are indicated.

(c) RT-PCR shows that the *XRCC1* mRNA is present in wild-type (+/+) and heterozygous (+/-) plants, but absent in the *xrcc1* mutant (-/-). Control amplification of RPL4 mRNA was used as a control for mRNA quality (left-most three lanes).

and the mutant allele shows normal Mendelian 1:2:1 segregation (34 *XRCC1 XRCC1* : 54 *XRCC1 xrcc1* : 30 *xrcc1 xrcc1*; χ^2 , 2 d.f. = 1.12; $P = 0.57$).

Polymerase chain reaction using primers within the gene and the T-DNA (o406–o599 and o406–o598; Figure 1b) showed that the T-DNA insertion in the mutant allele has two left borders (LBs) and is inserted in the short intron between the fifth and sixth exons of the *XRCC1* gene. Sequencing of the amplified T-DNA junctions shows a deletion of three nucleotides of the *XRCC1* gene at the insertion site (Figure 1a). Such double-LB T-DNA insertions are not uncommon among these insertion lines (for example see Bleuyard *et al.*, 2005).

Total RNA was isolated from *XRCC1/XRCC1*, *XRCC1/xrcc1* and *xrcc1/xrcc1* plants and semi-quantitative RT-PCR used to determine the presence or absence of native *XRCC1* transcripts. Amplification with primers spanning the insertion site (o598–o599) yielded the expected 419-nucleotide fragment with RNA prepared from heterozygote and wild-type plants. No *XRCC1* amplification product was detected in RNA from homozygote mutant plants, showing the absence of native *XRCC1* transcripts in the mutant. The weaker, higher molecular weight (866 bp) band corresponds to amplification of the genomic wild-type *XRCC1* gene due to the presence of some genomic DNA in the RNA preparation. As expected, this band was only seen in the wild-type and heterozygote samples (Figure 1c). That the three RNA

samples were of similar quality and concentration was verified by control amplification of the *RPL4* mRNA (359 nt).

Gamma-ray hypersensitivity

We have previously shown that absence of the AtKu80 protein reduces DNA end-joining activity by approximately two- to fourfold in an *in vivo* plasmid end-joining assay (Gallego *et al.*, 2003), in addition to conferring hypersensitivity to DSB-inducing agents (Tamura *et al.*, 2002; West *et al.*, 2002; Friesner and Britt, 2003; Gallego *et al.*, 2003). In order to test for a possible role of the AtXrcc1 protein in Arabidopsis DSB repair and whether or not it acts independently of the NHEJ pathway, we crossed the *xrcc1* and *ku80* mutant plants and screened F₂ progeny of this cross by PCR for wild-type, *ku80*, *xrcc1* and *ku80 xrcc1* mutant plants. F₃ seed was collected from these plants and used for the work presented here.

Five-day-old seedlings of the different genotypes were irradiated with different doses of γ -rays, and the plants were returned to the growth chamber. Representative images of the root tips of these plants 8 days post-irradiation are shown in Figure 2. Wild-type plantlets show little sensitivity up to 100 Gy, with radiosensitivity becoming clearly visible at 120 and 150 Gy. In contrast, development of roots of the *ku80* and *xrcc1* mutants is clearly affected at 80 and 100 Gy and far more severe developmental defects than those of wild-type plants are present at doses of 120 and 150 Gy. The roots show cell enlargement and the appearance of root hairs, and in more extreme cases emergence of a new root from tissue above the root tip due to the death of the meristem (Hefner *et al.*, 2006; Curtis and Hays, 2007; Fulcher and Sablowski, 2009). To detect killing of root meristematic cells we stained the different roots with propidium iodide 1 day after irradiation with 80 Gy. The *ku80*, *xrcc1* and *ku80 xrcc1* roots clearly show greater numbers of dead cells than the wild type (Figure 3). Thus, as for AtKu80, absence of AtXrcc1 confers hypersensitivity to γ -rays and in this qualitative assay *xrcc1* mutants appear even more sensitive to γ -rays than *ku80* mutant plants. Furthermore, the double *xrcc1 ku80* mutant plantlets are at least as sensitive as the single mutants.

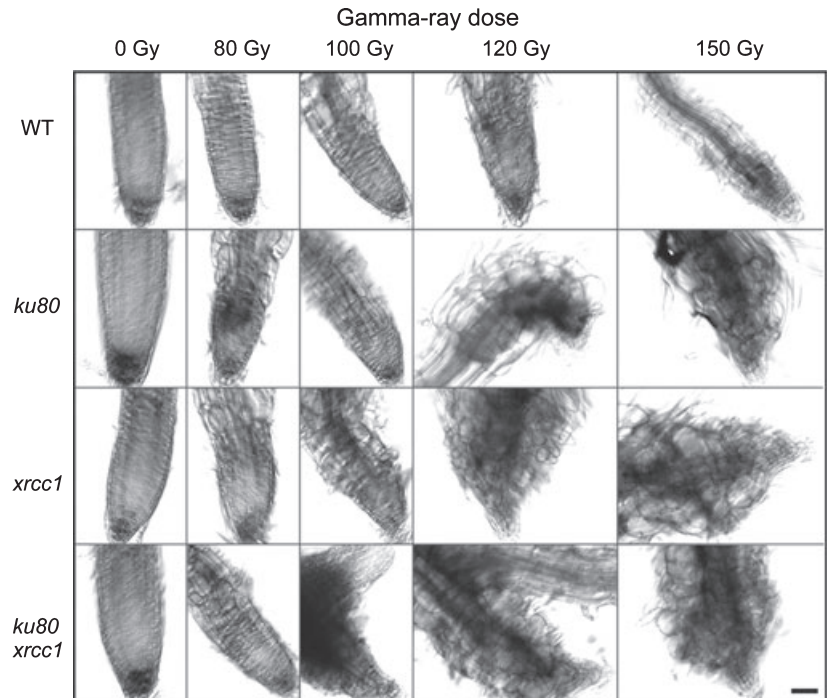
Kinetics of DNA DSB repair

The most probable explanation for the hypersensitivity of *xrcc1* plantlets to γ -rays is a defect in the repair of DNA damage in these plants. In order to determine whether this is specifically due to a defect in the repair of DNA DSB we have quantified the kinetics of DSB repair in dividing root tip cells of these plants by counting foci of the phosphorylated histone variant H2AX (γ -H2AX).

Phosphorylation of histone H2AX adjacent to DNA DSB sites is one of the earliest steps in the cascade of events in the cellular response to and repair of DSB (reviews by Branzei and Foiani, 2008; Kinner *et al.*, 2008; Shiloh, 2006).

Figure 2. Hypersensitivity of mutant plants to γ -radiation.

Five-day-old wild-type (WT) and mutant seedlings were γ -irradiated at 0, 80, 100, 120 and 150 Gy. Polarised brightfield images were taken 8 days after irradiation, each picture is an example of six roots. A 50 μ m scale bar is included in the lower right image.



The development of antisera to phospho-H2AX and the use of these for immunohistology has resulted in a powerful tool for the quantification of DNA breakage and repair in cells. As discussed in the recent review of Kinner *et al.* (2008), the counting of γ -H2AX foci has considerable advantages over alternative physical methods for detecting nuclear DNA breakage, in particular it permits the use of low, non-lethal levels of DNA damage and avoids possible artefactual production of DNA breaks by aggressive lysis and extraction procedures (e.g. conversion of heat-labile lesions to DSB; see Karlsson *et al.*, 2008; Rothkamm and Lobrich, 2003). It is important to note, however, that the loss of γ -H2AX foci measures the removal of γ -H2AX following removal of the signal leading to phosphorylation of H2AX (the DSB) and does not directly measure the completion of repair (Keogh *et al.*, 2006).

We have made an antiserum to *Arabidopsis* γ -H2AX following the methodology of Friesner *et al.* (2005) (see Experimental Procedures) and present here the use of this tool for quantitative kinetic analyses of DSB repair in root tip cells of irradiated *Arabidopsis* plantlets. As described in Experimental Procedures, this antiserum gives identical results in our hands to those found by the Britt group (Friesner *et al.*, 2005).

As previously described by Friesner *et al.* (2005), M-phase nuclei of *Arabidopsis* root tips show a linear dependence of the number of γ -H2AX foci on the γ -ray dose. These foci are dependent upon ataxia telangiectasia mutated (ATM) and ATM and Rad3-related (ATR) and no, or very rare, foci are detected in non-irradiated plants. We have thus analysed M-phase nuclei of young *Arabidopsis* plantlets. Given that

our detection window is restricted to the M-phase of the cell cycle, two further control experiments were necessary to validate the use of quantification of foci for kinetic analyses of DSB repair in the living root tips: verification of cell-cycle timing to determine the cell-cycle phase of nuclei at the time of irradiation, and measurement of the G₂/M-phase checkpoint to measure possible blockage of entry of damaged nuclei into M-phase in the context of our time courses.

In order to establish the position in the cell cycle of the nuclei at the time of irradiation, bromodeoxyuridine (BrdU) was added to growing plantlets immediately prior to irradiation – BrdU is incorporated into chromosomal DNA during S-phase and BrdU-positive nuclei can be detected after staining with the appropriate antiserum. Plantlets were then fixed after 1.5, 3, 6 and 24 h and stained for BrdU-DNA and with 4',6-diamidino-2-phenylindole (DAPI). Incorporation of BrdU was detected in interphase nuclei at all time points, but only at the 6 and 24 h time points in M-phase nuclei (Figure 4 and data not shown). As the first detectable BrdU-positive mitoses were found at the 6-h time point, with none detected in the 1.5 and 3 h samples, we can thus establish 3 h as the minimum length of the S + G₂ phase in these root tip cells. As our analysis focuses principally on the first 90 min post-irradiation, we can thus conclude that we are analysing 4C nuclei, having replicated their genomes at the time of irradiation.

An alternative explanation for the reduction of numbers of γ -H2AX foci in M-phase nuclei is that nuclei containing DSB are selectively prevented from entering the M-phase of the cell cycle by activation of the G₂/M phase cell-cycle checkpoint. Activation of cell-cycle checkpoints is a common

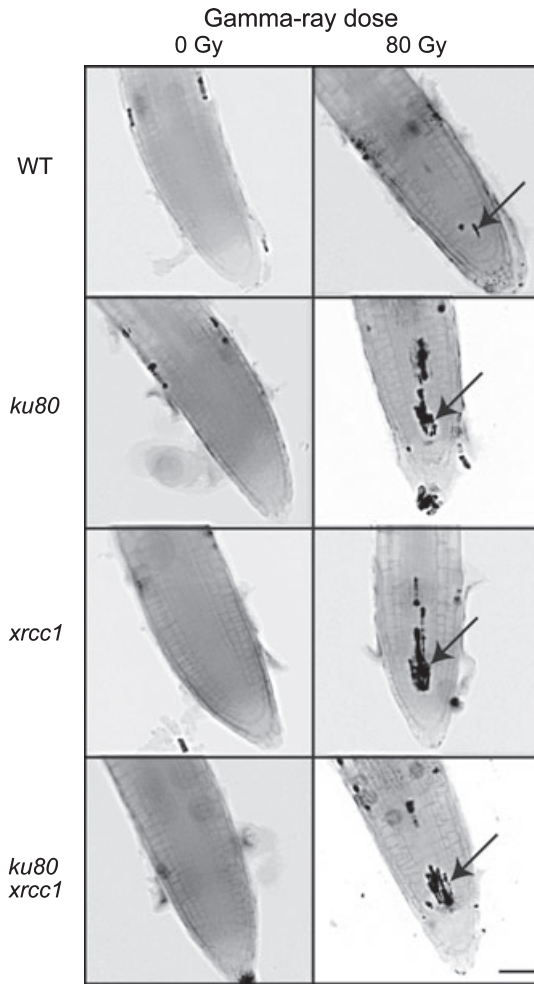


Figure 3. Cell death in γ -irradiated plants. Five-day-old seedlings were γ -irradiated at 80 Gy or not. The figure shows propidium iodide staining epifluorescence images of root tips 1 day after irradiation. Each image is an example of five stained roots. Black arrows show dead cells. A 50 μ m scale bar is included in the lower right image. WT, wild type.

feature of DNA damage response, and DNA-dependent activation of the G₂/M phase checkpoint has been described in Arabidopsis (Preuss and Britt, 2003; Culligan *et al.*, 2004; Hefner *et al.*, 2006). In order to verify the impact of this on our analysis, we measured the numbers of mitoses per root tip in wild-type and mutant plantlets across our time course, at 0, 10, 20, 45, 90 and 180 min after irradiation (Figure 5). No detectable G₂/M blockage is seen up to the 45 min time point, with a clear reduction in the number of mitoses seen only at 90 and 180 min post-irradiation. In addition, no significant difference in mitotic activity is seen between the wild-type, *ku80*, *xrcc1* and *ku80 xrcc1* plantlets. These data thus confirm that activation of the G₂/M checkpoint does not significantly affect our quantification of γ -H2AX foci at time points up to 45 min post-irradiation. However, checkpoint activation may affect the measurements at later (90 and

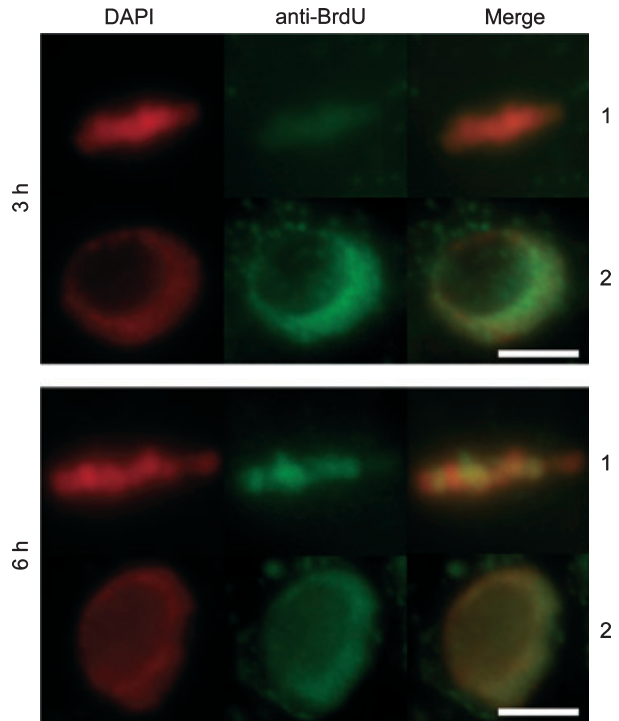


Figure 4. Timing of the G₂ phase. Five-day-old seedlings were placed in bromodeoxyuridine (BrdU)-containing medium and γ -irradiated at 25 Gy. After 1.5, 3, 6 and 24 h root tips were fixed and stained with 4',6-diamidino-2-phenylindole (DAPI) and for BrdU incorporation. Representative images of M-phase (1) and interphase (2) nuclei from 3-h (upper panel) and 6-h (lower panel) points are shown. The red is DAPI fluorescence and immunodetection of BrdU is green. Incorporation of BrdU is seen in interphase nuclei at both time points, but is first detected at the 6-h time point in M-phase nuclei. A 2.5 μ m scale bar is shown at the bottom right of each panel.

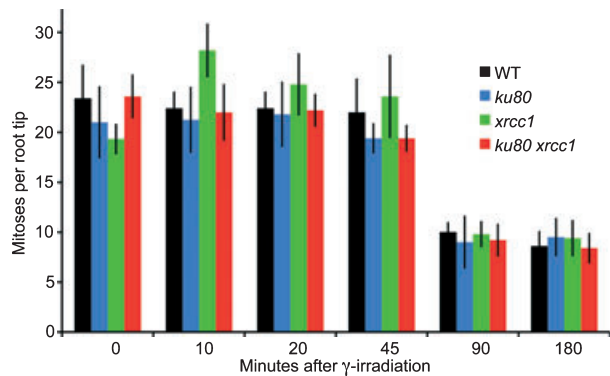


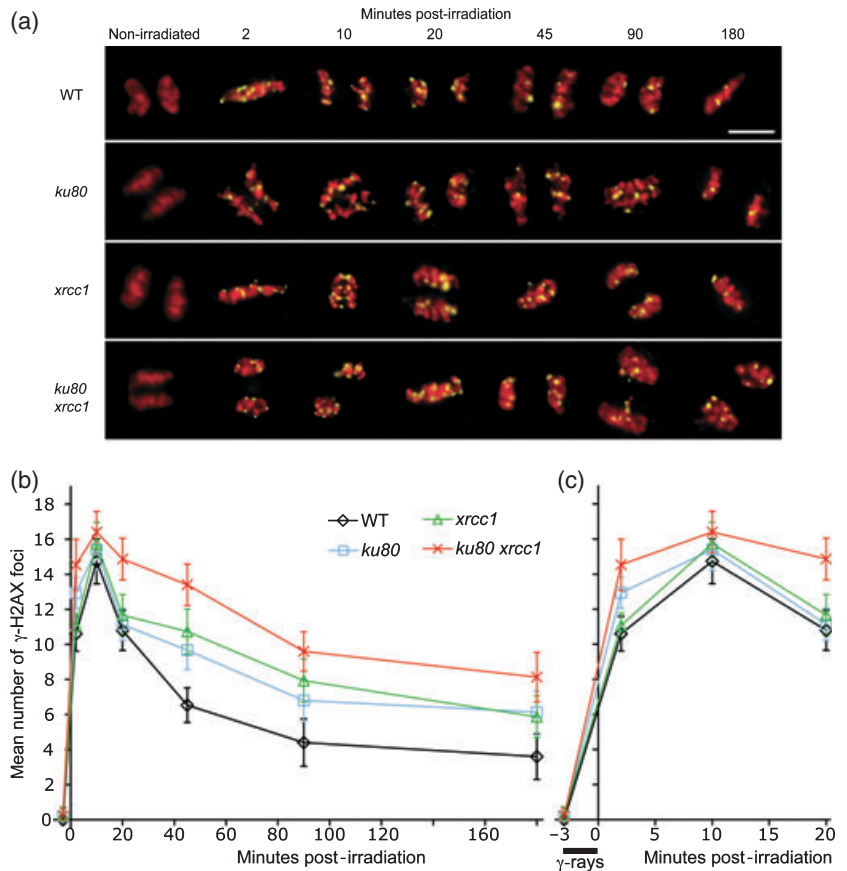
Figure 5. Mitotic activity following γ -irradiation. Measurement of mitotic activity following γ -irradiation. Five-day-old seedlings were fixed at different times after 25 Gy γ -rays. Fixed root tips were stained with 4',6-diamidino-2-phenylindole (DAPI) and the number of mitoses counted for each root tip. No reduction of mitotic activity is detected up to the 45 min time point. Plants of all four genotypes [wild type (WT), *ku80*, *xrcc1*, *ku80 xrcc1*] show a significant reduction in the number of mitoses at 90 min post-irradiation, indicative of activation of the G₂/M phase checkpoint. Values are means from five root tips for each genotype. Error bars are \pm 1 standard deviation.

Figure 6. Kinetics of γ -H2AX after γ -irradiation. Five-day-old wild-type (WT), *ku80*, *xrcc1* and *ku80 xrcc1* seedlings were γ -irradiated with 25 Gy and roots tips prepared for 4',6-diamidino-2-phenylindole (DAPI) and γ -H2AX immunostaining.

(a) Representative Z-stack projection images across the time courses with M-phase nuclei stained with DAPI in red and γ -H2AX foci in yellow. A 2 μ m scale bar is shown at the upper right.

(b) Numbers of γ -H2AX foci per M-phase nucleus of WT, *ku80*, *xrcc1* and *ku80 xrcc1*. Each point is the mean number of γ -H2AX foci per nucleus from counting 15 nuclei from 15 to 20 individual plantlets. Error bars are ± 1 standard deviation.

(c) A zoom of the first 20 min of the graph is shown in panel. The 3-min duration of the γ -irradiation is indicated by a bar under the graph.



180 min) time points, although this applies equally to the different genotypes and would thus not affect relative differences between the different mutants and the wild type.

In non-irradiated wild-type plantlets, 2% of root-tip M-phase nuclei (2/101) show one γ -H2AX focus and no nuclei were seen with more than one focus. As expected, these figures are higher in the unirradiated mutant plants: one focus in five nuclei and two foci in one nucleus in *ku80* (of 36 total); one focus in four nuclei and none with two foci in *xrcc1* (of 15 total); one focus in seven nuclei and none with two foci in *ku80 xrcc1* (of 25 total). The mean number of foci per non-irradiated M-phase nucleus remains low, however (maximum of 0.2 foci per nucleus), and does not affect the analysis of the irradiated plants.

Irradiation of wild-type Arabidopsis plantlets with 25 Gy results in approximately 15 γ -H2AX foci per M-phase nucleus (Figure 6a–c). The foci appear rapidly with a maximum of 10 min after irradiation and are then lost over time. The loss of the foci occurs rapidly over the 30 min following the maximum (approximately 50% of foci removed) and then continues more slowly with approximately 70% of foci removed 3 h after irradiation. Although the sampling is not sufficiently dense to draw conclusions concerning the linearity or exponentiality of the responses, more careful examination of the data shows three phases of DSB repair:

initial fast repair (up to 20 min), followed by a slower but rapid phase (up to 90 min) and finally, slow repair to the end of the time course. Identical results were found in experiments with two other wild-type lines from our collection (Figure S1 in Supporting Information).

DNA repair in the *ku80* and *xrcc1* mutant plantlets is clearly slower than in the wild type. Absence of either of these two proteins causes a repair defect appearing principally in the intermediate phase of repair (between 20 and 90 min after irradiation), with the initial rapid repair (up to 20 min) and the slow tail (after 90 min) being little affected. The situation is, however, very different in the double *xrcc1 ku80* mutant plants, which are considerably slower to repair the DSB and are strongly affected in both the initial rapid and intermediate slower repair phases. This non-epistatic relationship shows that Xrcc1 is required for a Ku80-independent DSB repair pathway in Arabidopsis.

DISCUSSION

In this work we present the identification of an Xrcc1-dependent, Ku-independent, DSB repair pathway in plants. This conclusion comes both from standard radiosensitivity data and on the kinetics of loss of γ -H2AX foci in dividing cells of living Arabidopsis plants. We present an analysis of the kinetics of DNA DSB repair in dividing G₂/M phase root

tip cells of plants and its use to analyse DSB repair pathways *in planta*.

As described in the Introduction, the first identified pathway of NHR was NHEJ. This is initiated by the recognition and binding of the broken DNA ends by the Ku heterodimer, Ku70 and Ku80, followed by processing of the ends by Artemis and Pol-X polymerases and ligation by ligase 4, Xrcc4 and XLF (reviewed by Bleuyard *et al.*, 2006; Lieber, 2008). However, NHEJ does not account for all end-joining repair of DSBs in living cells, and studies in recent years have shown the existence of two other NHR pathways in addition to Ku-dependent 'classical' or C-NHEJ, namely MMEJ and A-NHEJ.

Based on DNA sequence homology an orthologue of the *XRCC1* gene is clearly identifiable in the Arabidopsis genome (Uchiyama *et al.*, 2008). A recent study has identified the equivalent gene in rice (*OsXRCC1*) and shown that the protein interacts with both ss- and ds-DNA *in vitro* and with OsPCNA *in vitro* and *in vivo* (Uchiyama *et al.*, 2008). We thus identified, obtained and characterised an Arabidopsis line carrying a T-DNA insertion in the putative *XRCC1* gene. The insertion allele was characterised and the mutant line shown to carry a non-functional mutant *xrcc1* allele. The mutant allele segregates as a single Mendelian character and homozygous mutant plants show apparently normal development and are fully fertile. Homozygous *xrcc1* mutant plants are hypersensitive to γ -rays and this hypersensitivity is at least as strong as that of *ku80* mutants. Double mutant *ku80 xrcc1* plants are at least as γ -hypersensitive as the *xrcc1* mutants; however, as discussed below, the complexity and relative imprecision of survival measurements in plant radiobiology make it difficult to give quantitative judgements concerning epistasis. Propidium iodide staining confirmed the hypersensitivity of the mutants, showing killing of dividing meristematic cells of the mutants at lower γ -ray doses than for wild-type plants. We have thus characterised an *xrcc1* mutant of Arabidopsis and shown that absence of the Xrcc1 protein confers radiosensitivity in Arabidopsis.

Gamma-rays induce a range of lesions in cellular DNA, and notwithstanding the importance of the repair of DSB for survival, hypersensitivity could be due to defects in repair pathways other than DSB repair. The use of radiosensitivity data to analyse DNA repair in plants is complicated by the fact that although it is possible to detect killing of dividing cells in plant meristems (Figure 3; Curtis and Hays, 2007; Fulcher and Sablowski, 2009; Ricaud *et al.*, 2007), such radio-induced cell death does not translate simply to death of the plant. It has been assumed that this is the result of the nature of plant development, with the death of individual dividing meristematic cells being compensated by division of their sisters and at most leading to a temporary slowing of the plant's growth. Very high doses must be used in order to see killing of the whole plant and, given their sessile nature, this considerable radio-resistance of plants with respect to

animals is very probably a characteristic favoured by natural selection. By quantifying numbers of DNA breaks per nucleus in mitotically active cells, we have taken a different approach that permits working at doses producing physiologically relevant amounts of damage. For practical reasons, our experiments have been carried out at 25 Gy of ^{137}Cs γ -rays. This dose produces approximately 15 DSB per 4C G₂/M phase nucleus, or 0.56 foci Gy⁻¹ in Arabidopsis root tip cells. As these cells contain approximately 500 Mbp of DNA, a simple calculation results in a figure of 1.12 DSB Gy⁻¹ Gbp⁻¹. As discussed by Friesner *et al.* (2005), this figure is lower than published values of 2 for tobacco cells and 5–6 for yeast and vertebrate cells (Cedervall *et al.*, 1995; Prise *et al.*, 1998; Rothkamm and Lobrich, 2003; Yokota *et al.*, 2005), although other reports give a greater spread of values, with 2.64–17.8 DSB Gy⁻¹ Gbp⁻¹ reported for *Escherichia coli*, *Deinococcus radiodurans*, yeast, Chinese hamster ovary (CHO) and mouse cells (Resnick and Martin, 1976 and references therein). Given the use of different experimental systems and cell types and the rapid kinetics of DSB repair, we feel that it is premature to draw conclusions from these differences at this time. An illustration of the possible importance of the rapid kinetics of repair on measured values of DSB Gy⁻¹ Gbp⁻¹ is seen in the analyses presented below.

The appearance of γ -H2AX foci in dividing Arabidopsis root cells is very rapid, showing a strong peak 10 min post-irradiation (Figure 6b,c). That this peak reflects the competing effects of the establishment and removal of γ -H2AX foci is suggested both by the absence of a plateau in the number of foci and that the peak is higher in the repair defective mutant lines: *ku80* and *xrcc1* mutants show a higher peak than the wild-type and the double mutant an even higher peak. Interestingly this situation may differ in mammalian cells, which show an approximately hour-long plateau in the number of foci after their initial rapid appearance (Kinner *et al.*, 2008).

Three phases are visible in our analyses of the kinetics of DSB repair of γ -ray-induced DSBs in dividing Arabidopsis root tip cells. After a phase of very rapid repair in the first 20 min, a second less rapid phase is seen lasting up to 45 min post-irradiation and finally a slow repair process continues beyond this. Interpretation of time points beyond 45 min post-irradiation must, however, take into account our observation of a reduction in the mitotic activity in the root tips between the 45 and 90 min time points. This is presumably due to the activation of the G₂/M checkpoint, shown to function in Arabidopsis (Preuss and Britt, 2003; Culligan *et al.*, 2004; Hefner *et al.*, 2006), and could act to block entry of more damaged nuclei to the M-phase detection window.

The absence of Ku80 in *ku80* mutant plants significantly reduces repair in the second (20–45 min) phase and increases the number of foci detected at the 2-min point

during the accumulation phase, clearly demonstrating a role for AtKu80 in the first minutes following γ -irradiation. It is interesting to compare these results with the comet assay-based kinetics analysis recently published for Arabidopsis (Kozak *et al.*, 2009). This study analysed the repair of bleomycin-induced DSB in Arabidopsis plantlets using the neutral comet assay which provides an indirect physical measurement of genome fragmentation. A strong DSB repair defect was seen in the Arabidopsis *rad21* and *mim* (SMC6 orthologue) cohesion mutants. As is the case with the γ -H2AX data presented here, rapid repair kinetics were reported in this study; however, the *ku80* (and *lig4*) mutant surprisingly showed even more rapid repair than the wild type. It seems probable that these apparently divergent results arise from differences in the cell types studied – the comet assay measures nuclei from a mixed population of cell types and cell-cycle phases, with presumably a majority of non-cycling cells. It is also possible that the extraction procedure and differences between bleomycin treatment (1 h, unknown number of DSBs) and the γ irradiation (3 min, 15 DSBs per 4C nucleus) as well in the effective doses used may have affected quantification of the early time points in the comet assay and so masked the role of AtKu80.

As with the *ku80* mutant, *xrcc1* mutant plants also show a significant reduction in the efficiency of DSB repair in the second repair phase. The hypersensitivity to γ -rays of the *xrcc1* mutant plants is associated with a defect in DSB repair. These data thus confirm the existence of an Xrcc1-dependent DSB repair pathway in Arabidopsis acting in the second, 20–45 min, repair phase. However, in contrast to the *ku80* mutant, *xrcc1* plants show no increase in the number of DSBs at the 2-min time point, suggesting either that this pathway plays no role in the first minutes following irradiation or that its role can be compensated for by the Ku-dependent pathway.

That the *ku80* and *xrcc1* mutants define the existence of two separate DSB pathways was confirmed by analysing the double, *ku80 xrcc1*, mutant. As seen in Figure 6, *ku80* and *xrcc1* mutants are clearly not epistatic, with the double mutant plants showing significantly more severe repair defects at time points up to 45 min post-irradiation. The number of foci in *ku80 xrcc1* at the 2-min point is clearly greater than that of *ku80* (*t*-test, $P = 6.9 \times 10^{-3}$), which is higher than in *xrcc1* and the wild type (*t*-test, $P = 8.0 \times 10^{-6}$). This observation clearly suggests that Xrcc1 plays a role in repair in the first minutes following irradiation in the absence of Ku80, but not in its presence. This action of Ku, and more generally the importance of C-NHEJ in blocking the activity of alternative end-joining, has recently been reported in human and mouse cells (Boboila *et al.*, 2010; Fattah *et al.*, 2010; Simsek and Jasin, 2010). Notwithstanding this, we also observe a clear DNA DSB repair defect in *xrcc1* Arabidopsis, in the presence of Ku.

In conclusion, we have established the kinetics of DSB repair of γ -ray-induced DNA DSBs in G₂/M phase mitotic cells of the living Arabidopsis root tip. Using *ku80*, *xrcc1* and *ku80 xrcc1* mutants, we show that these two proteins define individual, non-epistatic DSB repair pathways and show a role for Ku in the first minutes post-irradiation. Furthermore, we show that Xrcc1 also plays such a role, but only in the absence of Ku. This new analysis thus provides the functional demonstration of the existence in plants of Xrcc1-dependent DSB repair and presumably the A-NHEJ pathway in plants. Given the notable absence of DNA ligase III in the annotated Arabidopsis genome, this raises the question of which DNA ligase is involved in the Xrcc1-dependent pathway. We also note that the kinetics clearly indicate the existence of other DSB repair pathways in these cells, and we are currently extending these studies to test the roles of homologous recombination pathways in plant DSB repair.

EXPERIMENTAL PROCEDURES

Growth

Seeds were surface-sterilised with 7% (w/v) calcium hypochlorite for 15 min and rinsed four times with sterile water. Seeds were sown on Petri plates containing 1× Murashige and Skoog (MS) medium including vitamins and 2-(*N*-morpholine)-ethanesulphonic acid (MES) buffer (no. M0255; Duchefa Biochemie, <http://www.duchefa.com/>), plus 3% sucrose (Duchefa), solidified with 0.8% agar (Bacto-Agar, DIFCO, Becton Dickinson Co., <http://catalog.bd.com>). Approximately 50 seeds were sown, well separated, on each plate. Petri dishes were placed at 4°C overnight (15 h) and transferred to a growth chamber (16 h light, 8 h dark, 23°C).

Plant lines

The T-DNA insertion Arabidopsis *ku80* mutant has been described previously (Gallego *et al.*, 2003). In this work we describe a *xrcc1* T-DNA insertional mutant from the SALK collection (Alonso *et al.*, 2003). *ku80* and *xrcc1* plants were crossed to obtain the *ku80 xrcc1* double mutant plant line. Wild-type and mutant plants used in this study are from lines derived from F₂ progeny of this cross.

PCR genotyping

The mutant *xrcc1* allele was identified by PCR genotyping. Primer combinations used to amplify the wild-type *XRCC1* (*At1G80420*) locus were o598 (5'-CTTATGCATGCTGGAAAACCA-3') and o599 (5'-GACGATTCCATCTTCCAAGC-3') and the mutant *xrcc1* locus were o598 (or o599) and o406 (5'-GCGTGGACCGCTTGCTGCAACT-3', o406 is the LBb1 Salk T-DNA line primer). The PCR conditions were 15 min at 94°C followed by 28 cycles of 94°C, 30 sec; 58°C, 30 sec; 72°C, 90 sec. The PCR genotyping conditions for the *KU80* and *ku80* alleles have been described previously (Gallego *et al.*, 2003).

Semi-quantitative RT-PCR

For semi-quantitative RT-PCR, total RNA was extracted from 7-day-old wild-type, *XRCC1/xrcc1* heterozygote and *xrcc1/xrcc1* mutant seedlings. The RT-PCR with primers o598 and o599 for *XRCC1* (see above) was performed with 3 µg total RNA using the Titan One Tube RT-PCR System (Roche Diagnostics, <http://www.roche.com/>), according to the manufacturer's instructions. RNA quality was

controlled by parallel amplifications of RPL4 (Chinchilla *et al.*, 2007) with primers rpl4-F (5'-GTGATAGGTCAGGTCAGGGAACAA-3') and rpl4-R (5'-CCACCCAACCACGAACTTCACGCGAGTC-3'). *XRCC1* PCR conditions were: 30 min at 50°C for reverse transcription, initial denaturation for 2 min at 94°C, and then amplification was performed for 50 cycles (45 sec, 94°C; 30 sec, 62°C; 45 sec, 68°C). The same conditions were used for *RPL4*, except that the annealing step was at 58°C.

Gamma irradiation

Five-day-old seedlings were γ -irradiated using a ^{137}Cs source (C.I.S. Bio, Gif sur Yvette, France) at an absorbed dose rate of 8.3 Gy min⁻¹, and then replaced in the growth chamber.

γ -H2AX antibodies

An antiserum was raised and purified by Eurogentec S.A (<http://www.eurogentec.com/>) against a phospho-specific Arabidopsis H2AX peptide following the method published by the Britt group (Friesner *et al.*, 2005). Using a sample of antiserum kindly sent by Anne Britt, we have verified that this new antiserum gives identical results in our hands to that published by the Britt lab (Friesner *et al.*, 2005), with a dose of 25 Gy from a ^{137}Cs source inducing a mean of 15 γ -H2AX foci per 4C M-phase root nucleus in wild-type plants. Only rare foci are observed in non-irradiated wild-type plants (see text).

Microscopy

A motorised AxioImager.Z1 (Carl Zeiss AG, <http://www.zeiss.com/>) epifluorescence microscope was used to image root tips and mitotic nuclei. The microscope is equipped with an AxioCam Mrm camera and appropriate Zeiss filter sets for the fluorochromes used in this work (filter no. 49 – DAPI; no. 38HE – Alexa488; no. 47HE – propidium iodide). Captured images were further processed and enhanced using ADOBE PHOTOSHOP software (<http://www.adobe.com/>).

Cell death

One day after irradiation, seedlings were immersed in propidium iodide solution (5 $\mu\text{g ml}^{-1}$ in water) for 1 min and rinsed three times with water. Root tips were then transferred to slides in a drop of water and covered with a coverslip for microscopy observation (adapted from Curtis and Hays, 2007).

Root phenotype

Eight days after irradiation, primordial root tips were transferred to slides in a drop of water and covered with a coverslip for bright field microscopy observation.

γ H2AX kinetics

Slide preparation. Root tips were prepared as described (Liu *et al.*, 1993; Friesner *et al.*, 2005) with minor modifications: root tips were fixed for 45 min in 4% paraformaldehyde in PME [50 mM piperazine-*N,N'*-bis(2-ethanesulphonic acid) (PIPES), pH 6.9; 5 mM MgSO₄; 1 mM EGTA] and then washed 3 × 5 min in PME. Root tips were digested for 30 min in 1% (w/v) cellulase, 0.5% (w/v) cytohe-licase, 1% (w/v) pectolyase (Sigma, <http://www.sigmaaldrich.com/>, refs C1794, C8274, P5936) prepared in PME and then washed 3 × 5 min in PME. They were then squashed gently onto slides as described (Liu *et al.*, 1993), air dried and stored at -80°C.

Immunostaining. Immunostaining was performed as described (Friesner *et al.*, 2005) with the following modifications. Each slide was incubated overnight at 4°C with 50–100 μl rabbit, anti-plant

γ -H2AX antiserum diluted 1:600 in fresh blocking buffer (3% BSA, 0.05% Tween-20 (Sigma) in 1× PBS). Slides were washed 3 × 5 min in 1× PBS solution and then incubated for 2–3 h at room temperature in 50–100 μl blocking buffer consisting of Alexa 488-conjugated goat anti-rabbit (1:1000, Molecular Probes, Invitrogen, <http://www.invitrogen.com>) secondary antibodies. Finally, slides were washed 3 × 5 min in PBS and mounted in Vectashield mounting medium with DAPI (1.5 $\mu\text{g ml}^{-1}$) (Vector Laboratories Inc., <http://www.vectorlabs.com/>).

Counting of γ -H2AX foci. Three-dimensional image stacks were treated with the ZEISS AXIOVISION 4.6.2 (<http://www.zeiss.com/>) deconvolution module (theoretical PSF, iterative algorithm) and γ -H2AX foci were counted by eye. The images presented in Figure 4 are collapsed Z-stack projections obtained using the extended-focus module (projection method) of the axiovision software.

BrdU incorporation

One day before irradiation, seedlings were immersed overnight in nutritive solution: MS + vitamins, pH 5.7 (see above) and 3% sucrose. Just before irradiation, seedlings were transferred to the same nutritive solution with 10 μM BrdU and replaced in the growth chamber. At different time points, root tips were fixed, digested, squashed onto slides, dried and placed at -80°C, as described above for 'Slide preparation'.

Immunodetection was performed with the BrdU Labelling and Detection Kit (Roche) following the manufacturer's instructions. Briefly, slides were rehydrated and washed 3 × 5 min with Washing buffer; 50–100 μl of anti-BrdU solution applied to each slide for 30 min at 37°C; slides were washed 3 × 5 min with Washing buffer and each slide incubated with 50–100 μl of anti-mouse Ig-fluorescein secondary antibody for 30 min at 37°C. Finally, slides were washed 3 × 5 min in Washing buffer and mounted in Vectashield with DAPI as described above.

ACKNOWLEDGEMENTS

We thank the members of the recombination group for their help and discussions and Anne Britt for kindly sending a sample of anti- γ H2AX serum. The Etablissement Français du Sang and the service of Dr Fabrigly is thanked for access to the ^{137}Cs irradiator. This work was partly financed by an European Union research grant (LSHG-CT-2005-018785), a French Government ANR grant (ANR-07-BLAN-0068), the Centre National de la Recherche Scientifique, the Université Blaise Pascal, the Université d'Auvergne and the Institut National de la Santé et la Recherche Médicale. CC was supported by a MENRT doctoral fellowship.

SUPPORTING INFORMATION

Additional supporting information may be found on the online version of this article:

Figure S1. Kinetics of γ -H2AX after γ -irradiation.

Please note: As a service to our authors and readers, this journal provides supporting information supplied by the authors. Such materials are peer-reviewed and may be re-organized for online delivery, but are not copy-edited or typeset. Technical support issues arising from supporting information (other than missing files) should be addressed to the authors.

REFERENCES

- Ahmad, A., Robinson, A.R., Duensing, A., van Drunen, E., Beverloo, H.B., Weisberg, D.B., Hastly, P., Hoeijmakers, J.H. and Niedernhofer, L.J. (2008) ERCC1-XPF endonuclease facilitates DNA double-strand break repair. *Mol. Cell. Biol.* **28**, 5082–5092.

- Alonso, J.M., Stepanova, A.N., Leisse, T.J. *et al.* (2003) Genome-wide insertional mutagenesis of *Arabidopsis thaliana*. *Science*, **301**, 653–657.
- van Attikum, H., Bundock, P., Overmeer, R.M., Lee, L.Y., Gelvin, S.B. and Hooykaas, P.J. (2003) The *Arabidopsis* AtLIG4 gene is required for the repair of DNA damage, but not for the integration of *Agrobacterium* T-DNA. *Nucleic Acids Res.* **31**, 4247–4255.
- Audebert, M., Salles, B. and Calsou, P. (2004) Involvement of poly(ADP-ribose) polymerase-1 and XRCC1/DNA ligase III in an alternative route for DNA double-strand breaks rejoining. *J. Biol. Chem.* **279**, 55117–55126.
- Audebert, M., Salles, B. and Calsou, P. (2008) Effect of double-strand break DNA sequence on the PARP-1 NHEJ pathway. *Biochem. Biophys. Res. Commun.* **369**, 982–988.
- Babiychuk, E., Cottrill, P.B., Storozhenko, S., Fuangthong, M., Chen, Y., O'Farrell, M.K., Van Montagu, M., Inze, D. and Kushnir, S. (1998) Higher plants possess two structurally different poly(ADP-ribose) polymerases. *Plant J.* **15**, 635–645.
- Bleuyard, J.Y., Gallego, M.E., Savigny, F. and White, C.I. (2005) Differing requirements for the *Arabidopsis* Rad51 paralogs in meiosis and DNA repair. *Plant J.* **41**, 533–545.
- Bleuyard, J.Y., Gallego, M.E. and White, C.I. (2006) Recent advances in understanding of the DNA double-strand break repair machinery of plants. *DNA Repair (Amst.)*, **5**, 1–12.
- Boboila, C., Yan, C., Wesemann, D.R., Jankovic, M., Wang, J.H., Manis, J., Nussenzweig, A., Nussenzweig, M. and Alt, F.W. (2010) Alternative end-joining catalyzes class switch recombination in the absence of both Ku70 and DNA ligase 4. *J. Exp. Med.* **207**, 417–427.
- Bonato, D., Revers, L.F., Brendel, M. and Henriques, J.A. (2005) The eukaryotic Pso2/Snm1/Artemis proteins and their function as genomic and cellular caretakers. *Braz. J. Med. Biol. Res.* **38**, 321–334.
- Branzei, D. and Foiani, M. (2008) Regulation of DNA repair throughout the cell cycle. *Nat. Rev. Mol. Cell Biol.* **9**, 297–308.
- Caldecott, K.W. (2003) XRCC1 and DNA strand break repair. *DNA Repair (Amst.)*, **2**, 955–969.
- Cedervall, B., Wong, R., Albright, N., Dynlacht, J., Lambin, P. and Dewey, W.C. (1995) Methods for the quantification of DNA double-strand breaks determined from the distribution of DNA fragment sizes measured by pulsed-field gel electrophoresis. *Radiat. Res.* **143**, 8–16.
- Chinchilla, D., Zipfel, C., Robatzek, S., Kemmerling, B., Nurnberger, T., Jones, J.D., Felix, G. and Bolter, T. (2007) A flagellin-induced complex of the receptor FLS2 and BAK1 initiates plant defence. *Nature*, **448**, 497–500.
- Cordoba-Canero, D., Morales-Ruiz, T., Roldan-Arjona, T. and Ariza, R.R. (2009) Single-nucleotide and long-patch base excision repair of DNA damage in plants. *Plant J.* **60**, 716–728.
- Culligan, K., Tissier, A. and Britt, A. (2004) ATR regulates a G2-phase cell-cycle checkpoint in *Arabidopsis thaliana*. *Plant Cell*, **16**, 1091–1104.
- Curtis, M.J. and Hays, J.B. (2007) Tolerance of dividing cells to replication stress in UVB-irradiated *Arabidopsis* roots: requirements for DNA translesion polymerases eta and zeta. *DNA Repair (Amst.)*, **6**, 1341–1358.
- Doucet-Chabeaud, G., Godon, C., Brutescu, C., de Murcia, G. and Kazmaier, M. (2001) Ionising radiation induces the expression of PARP-1 and PARP-2 genes in *Arabidopsis*. *Mol. Genet. Genomics*, **265**, 954–963.
- Fattah, F., Lee, E.H., Weisensel, N., Wang, Y., Lichter, N. and Hendrickson, E.A. (2010) Ku regulates the non-homologous end joining pathway choice of DNA double-strand break repair in human somatic cells. *PLoS Genet.* **6**, e1000855.
- Feldmann, E., Schmiemann, V., Goedecke, W., Reichenberger, S. and Pfeiffer, P. (2000) DNA double-strand break repair in cell-free extracts from Ku80-deficient cells: implications for Ku serving as an alignment factor in non-homologous DNA end joining. *Nucleic Acids Res.* **28**, 2585–2596.
- Friesner, J. and Britt, A.B. (2003) Ku80- and DNA ligase IV-deficient plants are sensitive to ionizing radiation and defective in T-DNA integration. *The Plant J* **34**, 427–440.
- Friesner, J.D., Liu, B., Culligan, K. and Britt, A.B. (2005) Ionizing radiation-dependent gamma-H2AX focus formation requires ataxia telangiectasia mutated and ataxia telangiectasia mutated and Rad3-related. *Mol. Biol. Cell*, **16**, 2566–2576.
- Fulcher, N. and Sablowski, R. (2009) Hypersensitivity to DNA damage in plant stem cell niches. *Proc. Natl Acad. Sci. USA*, **106**, 20984–20988.
- Gallego, M.E., Bleuyard, J.Y., Daoudal-Cotterell, S., Jallut, N. and White, C.I. (2003) Ku80 plays a role in non-homologous recombination but is not required for T-DNA integration in *Arabidopsis*. *Plant J.* **35**, 557–565.
- Gottlich, B., Reichenberger, S., Feldmann, E. and Pfeiffer, P. (1998) Rejoining of DNA double-strand breaks in vitro by single-strand annealing. *Eur. J. Biochem.* **258**, 387–395.
- Guirouilh-Barbat, J., Huck, S., Bertrand, P., Pirzio, L., Desmaze, C., Sabatier, L. and Lopez, B.S. (2004) Impact of the KU80 pathway on NHEJ-induced genome rearrangements in mammalian cells. *Mol. Cell*, **14**, 611–623.
- Heacock, M., Spangler, E., Riha, K., Puizina, J. and Shippen, D.E. (2004) Molecular analysis of telomere fusions in *Arabidopsis*: multiple pathways for chromosome end-joining. *EMBO J.* **23**, 2304–2313.
- Hefner, E., Huefner, N. and Britt, A.B. (2006) Tissue-specific regulation of cell-cycle responses to DNA damage in *Arabidopsis* seedlings. *DNA Repair (Amst.)*, **5**, 102–110.
- Karlsson, K.H., Radulescu, I., Rydberg, B. and Stenerlow, B. (2008) Repair of radiation-induced heat-labile sites is independent of DNA-PKcs, XRCC1 and PARP. *Radiat. Res.* **169**, 506–512.
- Keogh, M.-C., Kim, J.-A., Downey, M. *et al.* (2006) A phosphatase complex that dephosphorylates gammaH2AX regulates DNA damage checkpoint recovery. *Nature*, **439**, 497–501.
- Kinner, A., Wu, W., Staudt, C. and Iliakis, G. (2008) Gamma-H2AX in recognition and signaling of DNA double-strand breaks in the context of chromatin. *Nucleic Acids Res.* **36**, 5678–5694.
- Kozak, J., West, C.E., White, C., da Costa-Nunes, J.A. and Angelis, K.J. (2009) Rapid repair of DNA double strand breaks in *Arabidopsis thaliana* is dependent on proteins involved in chromosome structure maintenance. *DNA Repair (Amst.)*, **8**, 413–419.
- Kramer, K.M., Brock, J.A., Bloom, K., Moore, J.K. and Haber, J.E. (1994) Two different types of double-strand breaks in *Saccharomyces cerevisiae* are repaired by similar RAD52-independent, nonhomologous recombination events. *Mol. Cell Biol.* **14**, 1293–1301.
- Lepiniec, L., Babiychuk, E., Kushnir, S., Van Montagu, M. and Inze, D. (1995) Characterization of an *Arabidopsis thaliana* cDNA homologue to animal poly(ADP-ribose) polymerase. *FEBS Lett.* **364**, 103–108.
- Liang, F., Romanienko, P.J., Weaver, D.T., Jeggo, P.A. and Jasin, M. (1996) Chromosomal double-strand break repair in Ku80-deficient cells. *Proc. Natl Acad. Sci. USA*, **93**, 8929–8933.
- Liang, L., Deng, L., Nguyen, S.C., Zhao, X., Maulion, C.D., Shao, C. and Tischfield, J.A. (2008) Human DNA ligases I and III, but not ligase IV, are required for microhomology-mediated end joining of DNA double-strand breaks. *Nucleic Acids Res.* **36**, 3297–3310.
- Lieber, M.R. (2008) The mechanism of human nonhomologous DNA end joining. *J. Biol. Chem.* **283**, 1–5.
- Lieber, M.R. (2010) The mechanism of double-strand DNA break repair by the nonhomologous DNA end-joining pathway. *Annu. Rev. Biochem.* **79**, 181–211.
- Liu, B., Marc, J., Joshi, H.C. and Palevitz, B.A. (1993) A gamma-tubulin-related protein associated with the microtubule arrays of higher plants in a cell cycle-dependent manner. *J. Cell Sci.* **104**(Pt 4), 1217–1228.
- Ma, J.L., Kim, E.M., Haber, J.E. and Lee, S.E. (2003) Yeast Mre11 and Rad1 proteins define a Ku-independent mechanism to repair double-strand breaks lacking overlapping end sequences. *Mol. Cell Biol.* **23**, 8820–8828.
- Mahaney, B.L., Meek, K. and Lees-Miller, S.P. (2009) Repair of ionizing radiation-induced DNA double-strand breaks by non-homologous end-joining. *Biochem. J.* **417**, 639–650.
- Mimitou, E.P. and Symington, L.S. (2009) Nucleases and helicases take center stage in homologous recombination. *Trends Biochem. Sci.* **34**, 264–272.
- Molinier, J., Stamm, M.E. and Hohn, B. (2004) SNM-dependent recombinational repair of oxidatively induced DNA damage in *Arabidopsis thaliana*. *EMBO Rep.* **5**, 994–999.
- Moore, J.K. and Haber, J.E. (1996) Cell cycle and genetic requirements of two pathways of nonhomologous end-joining repair of double-strand breaks in *Saccharomyces cerevisiae*. *Mol. Cell Biol.* **16**, 2164–2173.
- Nussenzweig, A. and Nussenzweig, M.C. (2007) A backup DNA repair pathway moves to the forefront. *Cell*, **131**, 223–225.
- Preuss, S.B. and Britt, A.B. (2003) A DNA-damage-induced cell cycle checkpoint in *Arabidopsis*. *Genetics*, **164**, 323–334.
- Prise, K.M., Ahnstrom, G., Belli, M. *et al.* (1998) A review of dsb induction data for varying quality radiations. *Int. J. Radiat. Biol.* **74**, 173–184.
- Rass, E., Grabarz, A., Plo, I., Gautier, J., Bertrand, P. and Lopez, B.S. (2009) Role of Mre11 in chromosomal nonhomologous end joining in mammalian cells. *Nat. Struct. Mol. Biol.* **16**, 819–824.

- Resnick, M.A. and Martin, P. (1976) The repair of double-stranded breaks in the nuclear DNA of *Saccharomyces cerevisiae* and its genetic control. *Mol. Gen. Genet.* **143**, 119–129.
- Ricaud, L., Proux, C., Renou, J.P., Pichon, O., Fochesato, S., Ortet, P. and Montane, M.H. (2007) ATM-mediated transcriptional and developmental responses to gamma-rays in *Arabidopsis*. *PLoS ONE*, **2**, e430.
- Riha, K., Watson, J.M., Parkey, J. and Shippen, D.E. (2002) Telomere length deregulation and enhanced sensitivity to genotoxic stress in *Arabidopsis* mutants deficient in Ku70. *EMBO J.* **21**, 2819–2826.
- Roldan-Arjona, T. and Ariza, R.R. (2009) Repair and tolerance of oxidative DNA damage in plants. *Mutat. Res.* **681**, 169–179.
- Rothkamm, K. and Lobrich, M. (2003) Evidence for a lack of DNA double-strand break repair in human cells exposed to very low x-ray doses. *Proc. Natl Acad. Sci. USA*, **100**, 5057–5062.
- San Filippo, J., Sung, P. and Klein, H. (2008) Mechanism of eukaryotic homologous recombination. *Annu. Rev. Biochem.* **77**, 229–257.
- Scholl, R.L., May, S.T. and Ware, D.H. (2000) Seed and molecular resources for *Arabidopsis*. *Plant Physiol.* **124**, 1477–1480.
- Shiloh, Y. (2006) The ATM-mediated DNA-damage response: taking shape. *Trends Biochem. Sci.* **31**, 402–410.
- Shrivastav, M., De Haro, L.P. and Nickoloff, J.A. (2008) Regulation of DNA double-strand break repair pathway choice. *Cell Res.* **18**, 134–147.
- Simsek, D. and Jasin, M. (2010) Alternative end-joining is suppressed by the canonical NHEJ component Xrcc4-ligase IV during chromosomal translocation formation. *Nat. Struct. Mol. Biol.* **17**, 410–416.
- Sonoda, E., Hohegger, H., Saberi, A., Taniguchi, Y. and Takeda, S. (2006) Differential usage of non-homologous end-joining and homologous recombination in double strand break repair. *DNA Repair (Amst.)*, **5**, 1021–1029.
- Tamura, K., Adachi, Y., Chiba, K., Oguchi, K. and Takahashi, H. (2002) Identification of Ku70 and Ku80 homologues in *Arabidopsis thaliana*: evidence for a role in the repair of DNA double-strand breaks. *Plant J.* **29**, 771–781.
- Taylor, R.M., Thistlethwaite, A. and Caldecott, K.W. (2002) Central role for the XRCC1 BRCT I domain in mammalian DNA single-strand break repair. *Mol. Cell. Biol.* **22**, 2556–2563.
- Taylor, E.M., Cecillon, S.M., Bonis, A., Chapman, J.R., Povirk, L.F. and Lindsay, H.D. (2009) The Mre11/Rad50/Nbs1 complex functions in resection-based DNA end joining in *Xenopus laevis*. *Nucleic Acids Res.* **38**, 441–454.
- Uchiyama, Y., Suzuki, Y. and Sakaguchi, K. (2008) Characterization of plant XRCC1 and its interaction with proliferating cell nuclear antigen. *Planta*, **227**, 1233–1241.
- Wang, H., Rosidi, B., Perrault, R., Wang, M., Zhang, L., Windhofer, F. and Iliakis, G. (2005) DNA ligase III as a candidate component of backup pathways of nonhomologous end joining. *Cancer Res.* **65**, 4020–4030.
- Wang, M., Wu, W., Rosidi, B., Zhang, L., Wang, H. and Iliakis, G. (2006) PARP-1 and Ku compete for repair of DNA double strand breaks by distinct NHEJ pathways. *Nucleic Acids Res.* **34**, 6170–6182.
- Waterworth, W.M., Kozak, J., Provost, C.M., Bray, C.M., Angelis, K.J. and West, C.E. (2009) DNA ligase 1 deficient plants display severe growth defects and delayed repair of both DNA single and double strand breaks. *BMC Plant Biol.* **9**, 79.
- West, C.E., Waterworth, W.M., Jiang, Q. and Bray, C.M. (2000) *Arabidopsis* DNA ligase IV is induced by gamma-irradiation and interacts with an *Arabidopsis* homologue of the double strand break repair protein XRCC4. *Plant J.* **24**, 67–78.
- West, C.E., Waterworth, W.M., Story, G.W., Sunderland, P.A., Jiang, Q. and Bray, C.M. (2002) Disruption of the *Arabidopsis* AtKu80 gene demonstrates an essential role for AtKu80 protein in efficient repair of DNA double-strand breaks in vivo. *Plant J.* **31**, 517–528.
- Xie, A., Kwok, A. and Scully, R. (2009) Role of mammalian Mre11 in classical and alternative nonhomologous end joining. *Nat. Struct. Mol. Biol.* **16**, 814–818.
- Yokota, Y., Shikazono, N., Tanaka, A., Hase, Y., Funayama, T., Wada, S. and Inoue, M. (2005) Comparative radiation tolerance based on the induction of DNA double-strand breaks in tobacco BY-2 cells and CHO-K1 cells irradiated with gamma rays. *Radiat. Res.* **163**, 520–525.
- Zhang, X. and Paull, T.T. (2005) The Mre11/Rad50/Xrs2 complex and non-homologous end-joining of incompatible ends in *S. cerevisiae*. *DNA Repair (Amst.)*, **4**, 1281–1294.